New patterns of polymer blend miscibility associated with monomer shape and size asymmetry

Jacek Dudowicz and Karl F. Freed
The James Franck Institute and the Department of Chemistry, The University of Chicago, Chicago, Illinois 60637

Jack F. Douglas
Polymers Division, National Institute of Standards and Technology, Gaithersburg, Maryland 20899

(Received 24 January 2002; accepted 14 March 2002)

Polymer blends are formulated by mixing polymers with different chemical structures to create new materials with properties intermediate between those of the individual components. While Flory–Huggins (FH) theory explains some basic trends in blend miscibility, the theory *completely neglects* the dissimilarity in monomer structures that is central to the fabrication of real blends. We systematically investigate the influence of monomer structure on blend miscibility using a lattice cluster theory (LCT) generalization of the FH model. Analytic calculations are rendered tractable by restricting the theoretical analysis to the limit of incompressible and high molecular weight blends. The well-known miscibility pattern predicted by FH theory is recovered only for a limited range of monomer size and shape asymmetries, but additional contributions to the LCT entropy and internal energy of mixing for polymers with dissimilarly shaped monomers lead to *three additional blend miscibilty classes* whose behaviors are quite different from the predictions of classical FH theory. One blend miscibility class (class IV) exhibits a remarkable resemblance to the critical behavior of polymer solutions. In particular, the theta temperature for class IV blends is near a molecular weight insensitive critical temperature for phase separation, the critical composition is highly asymmetric, and the correlation length amplitude is significantly less than the chain radius of gyration. Experimental evidence for these new blend miscibility classes is discussed, and predictions are made for specific blends of polyolefins that should illustrate these new patterns of blend miscibility.
 [DOI: 10.1063/1.1476696]

I. INTRODUCTION

Many commercially important materials are blends of polymers having different chemical and physical characteristics, and the stability and state of dispersion of these multiphase materials are often crucial in their applications. Flory–Huggins (FH) theory[1,2] has long provided the basis for understanding the thermodynamic properties of blends, and the theory also represents an essential input into the analysis of blend scattering data[3] and into kinetic models of blend phase separation.[4]

While FH theory[1,2] explains some trends in the thermodynamics of polymer blends and solutions, the theory completely neglects the relationship between blend miscibility and the chemical structure of the polymer constituents. Given improvements in synthetic chemistry that enable unprecedented control of polymer microstructure,[5] a pressing need exists for a more molecularly oriented theory that predicts how the monomer structural asymmetry affects blend thermodynamic properties. Over 30 years ago, Flory noted[2] that while FH theory is rudimentary because of its neglect of the detailed structure of polymer chains, the development of a more refined theory must emerge at a considerable sacrifice of simplicity (both in form and application). Moreover, such a generalization would have doubtful practical value if it required the introduction of many ''arbitrary parameters'' that must be determined from fits to experimental data. Due to the uncertain existence of a theory that is simultaneously accurate in detail, comprehensive in scope, and computationally managable, Flory suggested that the best strategy for effectively extending the FH theory is to consider simplified models of ''reasonable generality'' that can determine essential aspects of how molecular characteristics influence the equilibrium properties of these complex liquid mixtures.

The problem of understanding the interrelation between molecular monomer structure and blend miscibility has been considered by several complementary methods. The lattice cluster theory, developed by Freed and co-workers,[6–10] directly addresses the effects of blend compressibility, chain semiflexibility, and differences in monomer shapes, sizes, and interactions on the blend critical behavior. [FH theory, which neglects these effects, is the leading order contribution in the lattice cluster theory (LCT).] The LCT generalization of FH theory provided the first explanation for the origin of the ''entropic'' portion a of the Flory interaction parameter χ in terms of differences in monomer shapes and sizes between the blend components. (Flory[2] and Koningsveld *et al.*[11] anticipated the presence of a and its physical origin, but the LCT directly determines a from monomer structures without the introduction of adjustable parameters.) The LCT has also explained[12,13] a number of measurements that are impossible to rationalize from FH theory (e.g., negative values of the χ parameter, the variation in the nature of the phase transition

with the microstructure of isotopic polybutadiene blends[13]) and has predicted[14,15] novel phenomena (e.g., pressure dependence of χ parameter,[14] ordering of diblock copolymers upon heating[15]) subsequently verified by experiments.[16,17] However, the majority of its applications have been restricted to numerical studies, since the theory is algebraically involved.

Schweizer, Curro, and co-workers[18] have adapted integral equation methods (PRISM), along with closures and approximations appropriate for modeling polymer fluids in their investigations of the factors controlling blend miscibility and blend structure. Their studies confirm many results of FH theory (e.g., scaling of the critical temperature T_c with chain length) and provide complementary insights into the molecular dependence of the Flory interaction parameter χ, especially the effects of chain stiffness, asymmetries in monomer interactions, etc. Perhaps the main impact of the PRISM and LCT lies in producing a rationale for understanding phenomenological extensions of FH theory (e.g., the presence of an ''entropic'' contribution to χ, the concentration dependence of χ, the role of equation of state effects, etc.). The complexity of the integral equation and lattice cluster theories, however, has so far limited their capacity to predict *general trends* in blend miscibility having as broad a scope as the classical FH theory.[1,2] Basically, these theories have provided a ''license'' to fit χ as a phenomenological parameter.

We also mention the continuous chain theory of blend miscibility developed by Fredrickson *et al.*[19] The theory treats athermal blends (having polyolefin blends in mind) and predicts χ to be purely entropic (an interesting contrast to FH theory where it is purely energetic) and to be primarily dependent on the difference between the ''packing lengths'' of the polymer blend components, where the packing length is defined as the ratio of the square of the chain radius of gyration to the chain volume. This work yields a rationalization of the important experimental finding that polymer blends with similar molecular structures tend to have greater miscibility.[20,21]

Shortcomings of the FH theory that have been revealed by its comparison with experiments and simulations[22–24] indicate areas where theoretical improvements are needed. Treating the interaction parameter χ as a purely phenomenological quantity, which absorbs all unknown information concerning blend miscibility, largely eliminates the predictive nature of the FH model. Experiments demonstrate the existence of patterns of miscibility that are quite unlike those predicted by FH theory, and these findings give helpful clues into necessary extensions of the FH model.

Comparison between experiment and FH theory has been favorable for blends whose components exhibit little difference between monomer structures. For example, small angle neutron scattering (SANS) measurements[25] for symmetric ($\lambda_N \approx 1$) isotopic blends have verified that the critical value of the FH interaction parameter χ scales in inverse proportionality to the polymerization index N, and semiquantitative agreement is obtained between the FH/RPA model and measurements of the Ginzburg number Gi in a blend of polyisoprene and poly(ethylene propylene).[26] However, the accord between the FH model and measurements deteriorates for ''real blends'' where there are appreciable differences between the monomer structures of the blend components. For example, the critical temperature T_c of blends of polystyrene with poly(vinyl methyl ether) ($\lambda_N \approx 3.5$) is relatively insensitive[27] to the magnitude of N, and the blend phase boundaries are often reported[27,28] to be asymmetric, even for ''symmetric'' blends ($\lambda_N \approx 1$), in contrast to expectations based on FH theory. A similar insensitivity of T_c to N has been found[29] for binary blends of polyisobutylene and several other polyolefins, where it is difficult to imagine that any ''specific interactions'' could be responsible for the observed dramatic deviations from FH theory. Polyolefin blends ($\lambda_N \approx 1$) studied by Bates *et al.*[30] also exhibit deviations of blend miscibility from the predictions of FH theory. All these ''anomalous'' behaviors are compared to the predictions of our theoretical approach in Sec. V.

The present paper develops a different strategy toward understanding trends in blend miscibility. We restrict our analysis to the incompressible, long chain limit systems in order to obtain a *fully analytic* theory that can relate essential patterns of miscibility to monomer structural asymmetry and, therefore, can predict analytically how monomer structure influences blend miscibility. (This simplified version[31] of the LCT has already been used by to explain a large body of experimental data for binary blends.) We systematicaly investigate *all miscibility patterns that emerge from the SLCT theory*, and this procedure yields a new classification of binary blend critical behavior and new patterns of polymer blend miscibility that are not described by FH theory. The new classification scheme (briefly presented in a recent communication[32]) naturally explains the occurrence of blend phase separation upon heating (within an *incompressible* model)[28] and predicts dramatic changes in the molecular mass dependence of the critical parameters (T_c, ϕ_c, Gi, etc.) even for blends with symmetric polymerization indices ($\lambda_N = 1$). The patterns of miscibility predicted by the SLCT are preserved in the more complex LCT theory, although there are quantitative changes appearing when the incompressibily assumption is lifted.[7,33,34] Since monomer asymmetry is often the norm in commercial blends and other multiphase fluid mixtures, our classification should have important implications for technology and biological science applications where complex liquid mixtures are often encountered.

Section II summarizes essential characteristics of polymer blends and polymer solutions that can be derive from FH theory. Section III provides a brief description of the free energy expression obtained from the simplified lattice cluster theory (SLCT), followed by a derivation of the critical conditions and equations for the second and third virial coefficients, the correlation length amplitude ξ_o, and the Ginzburg number. The four general categories of binary blend critical behavior are described in Sec. IV, while Sec. V presents comparisons with experiments. The FH estimate for the critical composition ϕ_c is shown to in error for blends displaying a lower critical solution temperature (LCST) phase diagram, while small shifts from the FH critical composition $\phi_c^{(\mathrm{FH})}$ may arise for upper critical solution temperature (UCST) blends. The discussion section provides a review of the limi-

tations of the simplified lattice cluster theory and briefly describes the wider range of blend miscibility patterns that emerge when lifting some assumptions of this theory (e.g., when including effects due to chain semiflexibility, compressibility, monomer interaction asymmetry, etc.).

II. FLORY–HUGGINS THEORY: REVIEW OF BASIC FEATURES

FH theory is based on a highly idealized model of polymer blends and polymer solutions, and much of its attraction and success derives from its simplicity. Notably, the theory assumes that the mixtures are incompressible and polymer chains are fully flexible. No distinction is made between polymers having different chemical structures, so that the theory does not differentiate between linear, branched, ring, comb, star, etc., polymers. While the monomer structural asymmetry in polymer systems is completely ignored, FH theory accounts for another fundamental type of molecular symmetry, the asymmetry of polymerization indices (N_1,N_2) between the constituents of the mixture. In particular, FH theory predicts a significantly different pattern of miscibility in blends where N_1 and N_2 are comparable to each other from that corresponding to polymer solutions where N_1 and N_2 differ considerably $(N_1 \gg N_2)$.

A. Miscibility of polymer blends

FH theory indicates that polymer blends are much less miscible than their small molecule (monomeric) counterparts because of the reduction of the entropy of mixing associated with the presence of chain connectivity. This limited blend miscibility is directly reflected in the dependence of the blend critical temperature T_c on the polymerization indices N_1 and N_2 of the blend components.[1,2] The critical temperature T_c scales linearly with the ''reduced'' polymerization index[1,3,23] $\bar{N}=N_1N_2/(N_1^{1/2}+N_2^{1/2})^2$, and this scaling simplifies to $T_c \sim N$ for ''symmetric'' blends $(N_1=N_2=N)$. FH theory also predicts that an asymmetry in polymerization indices $(\lambda_N \equiv N_2/N_1 \neq 1)$ leads to an asymmetrical critical composition ϕ_c and to asymmetrical phase boundaries. The well known FH formula $\phi_c^{(\mathrm{FH})} \equiv \phi_c^{(1)} = 1-\phi_c^{(2)} = \sqrt{\lambda_N}/(1+\sqrt{\lambda_N})$ reduces to $\phi_c = 1/2$ only when $N_1=N_2$. Note that $\phi_c^{(\mathrm{FH})}$ is independent of $\{N_i\}$ if the ratio λ_N is held fixed, a prediction readily subjected to experimental tests, although these tests are rarely considered (see Sec. V).

The description of other ''critical properties'' by FH theory requires the use of the random phase approximation (RPA).[3] In particular, the correlation length amplitude ξ_o, determining the extent of composition fluctuation, is derived as a compositionally weighted average of the radii of gyration $[R_g^{(i)}]$ for the blend components.[1,3] Hence, ξ_o becomes proportional to $N^{1/2}$ for ''symmetric'' blends.[1,3] On the other hand, the Ginzburg number Gi, which quantifies the width of the Ising-type critical region, diminishes with increasing N_1 and N_2. The FH theory scaling $\mathrm{Gi} \sim 1/N$ (for ''symmetric'' blends) implies the existence of a small critical region and provides the basis for claims that mean field theory should describe high molecular weight blends.[35,36]

Fluctuation effects limit the accuracy of mean field estimates of phase boundaries and critical properties. Monte Carlo simulations of Binder and co-workers[22,23] demonstrate, for instance, that the error in T_c evaluated from the FH theory is about 25% (for low molecular weight dense ''symmetric'' mixtures) and that compressibility effects can make the error even larger. The fluctuation correction $\Delta T = T_c^{(\mathrm{mf})} - T_c$ has been found[23] to decrease with N $(\Delta T \sim N^{-1/2})$, in accord with arguments by Holyst and Vilgis.[37] For finite chain lengths, the fluctuation corrections can be appreciable, and this fact should be kept in mind.

Although Monte Carlo simulations have indicated substantial fluctuation-induced errors in the FH estimate of T_c and other blend properties, FH theory has been judged ''successful'' [23,38] in describing important qualitative features of blend miscibility (e.g., $T_c \sim N$ and $\mathrm{Gi} \sim 1/N$).[22–24] (Similar conclusions to those obtained from Monte Carlo simulations have followed from PRISM calculations by Singh and Schweizer.[39]) We note, however, that these simulations assume that polymers have *identical* monomer structures, so the ''mapping'' [23] of real polymer blends onto the FH model is unclear, if possible at all.

B. Miscibility of polymer solutions

A strikingly different pattern of miscibility emerges from FH theory in the $\lambda_N \to 0$ limit, corresponding to polymer solutions. Polymer chain connectivity still leads to a diminished miscibility of polymer solutions relative to the miscibility of monomeric mixtures $(N_1=N_2=1)$, but this decrease in compatibility is less dramatic than that occurring for high molecular weight polymer blends. Increasing N_1, while keeping N_2 constant (e.g., $N_2=1$) causes T_c to approach the theta temperature T_θ (defined as the temperature at which the second virial coefficient vanishes for the polymer solution). Notably, T_c for high molecular weight polymer solutions $(N_1 \to \infty,\ N_2=1)$ is *independent* of N_1 and equals four times T_c for the monomeric mixture,[40] $T_c(N=1)$. This result is contrasted with the FH theory prediction that T_c for polymer blends increases proportional to N without bound. The large chain length asymmetry of polymer solutions is also responsible for highly asymmetric phase boundaries, as reflected in the highly asymmetrical critical composition which tends to zero when $\lambda_N \to 0$ $[\phi_c^{(\mathrm{FH})} \sim \lambda_N^{1/2}]$.

Polymer solutions and polymer blends also display appreciable differences in their osmotic and scattering properties. While FH theory predicts that with increasing polymer chain length, T_c for polymer solutions approaches T_θ, T_c, and T_θ for polymer blends are expected to be greatly separated, regardless of the molecular weights (in FH theory, $T_\theta = 4T_c$ when $N_1=N_2$). The scale of composition fluctuations is also predicted to be significantly smaller for polymer solutions than for polymer blends. Specifically, the correlation length amplitude ξ_o [see Eq. (24)] for polymer solutions scales within FH/RPA theory proportional to $N^{1/4}$ (i.e., to the *geometrical mean* of the solvent and polymer radii of gyration).[41] The scaling of ξ_o with N affects the N-dependence of many other basic properties of polymer solutions, such as surface tension, interfacial width in the two

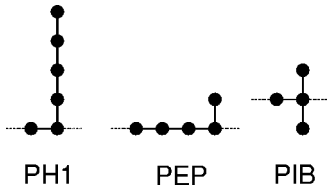

FIG. 1. United atom group models for monomers of poly(hexene-1) (PH1), poly(ethylene propylene) (PEP), and poly(isobutylene) (PIB). Circles designate CH_n groups, solid lines represent the C–C bonds inside the monomer, while dotted lines indicate the C–C bonds that link the monomer's CH_n groups with those belonging to other monomers in the polyolefin chain backbone. These three polyolefins are components of the two binary blends (PH1/PEP, PIB/PEP) chosen to illustrate non-FH-types of critical behavior that are predicted by the SLCT. Each blend component is characterized within the SLCT by two geometrical parameters r_i and p_i, and these parameters for these three polyolefins are $r_{\mathrm{PH1}}=7/6$, $p_{\mathrm{PH1}}=4/3$, $r_{\mathrm{PEP}}=p_{\mathrm{PEP}}=6/5$, $r_{\mathrm{PIB}}=7/4$, and $p_{\mathrm{PIB}}=3/2$. The differences $|r_1-r_2|$ and $|p_1-p_2|$ are measures of blend structural asymmetry.

phase regime, light and neutron scattering intensities, collective diffision coefficient, etc.

Fluctuation effects are especially large in polymer solutions, and the corrections to the mean field critical temperature $T_c^{(\mathrm{mf})}$ are comparable to those derived for small molecule liquids.[40] This arises regardless of arguments that Gi becomes small for polymer solutions.[37] Swelling of polymers in the vicinity of the solution theta temperature manifests an additional type of critical phenomena,[3,42,43] leading to nontrivial critical indices describing the interrelation between polymer size (R_g) and N, the concentration dependence of the osmotic pressure, etc. Moreover, de Gennes[3,44] has suggested that the critical behavior of polymer solutions is *tricritical* rather than Ising-type in the $\lambda_N \rightarrow 0$ limit since T_c is expected to approach T_θ. Evidence supporting this conjecture has recently been reported.[45] Although arguments and findings relating to fluctuation effects in polymer solutions lie beyond mean field theory, they serve to illustrate the large potential impact of molecular asymmetry (chain length asymmetry) on the critical behavior of fluid mixtures. Even the *qualitative* type of critical behavior may be influenced by molecular asymmetry if the de Gennes conjecture is proven correct.

III. SIMPLIFIED LATTICE CLUSTER THEORY OF BLEND MISCIBILITY

The lattice cluster theory (LCT) (Refs. 6, 7, 31) is based on two major improvements beyond the zeroth order FH theory. The first improvement lies in the use of united atom models to represent individual monomers that are described as occupying several neighboring lattice sites. Figure 1 illustrates united atom group models for a few polyolefins considered in this paper. The individual CH_n ($n=0-3$) groups are taken in these models as covering single lattice sites. Thus, the monomers can assume a wide range of shapes and sizes, subject to the constraint of a discrete lattice representation for these structures. The second improvement of the LCT involves a superior solution to the resulting lattice model. The FH free energy is the leading order approximation in the LCT, and corrections arising from chain connectivity, asymmetries in monomer–monomer interactions, and from short-range correlations emerge from a high temperature cluster expansion in powers of reciprocal dimensionality and the dimensionless van der Waals interaction energies.[6] A full account of the LCT is provided in our previous papers,[6,7] and here we focus on the general types of phase behavior predicted by a simplified version of the LCT for binary polymer mixtures.

The full LCT involves lengthy analytic expressions, and the task of classifying the general types of blend phase diagrams can only be achieved using numerical analysis. On the other hand, the availability of an analytically tractable, high pressure, high molecular weight limit of the LCT simplifies this task enormously.[31] An additional argument for the use of this simplified LCT (previously termed "the pedestrian LCT") emerges from our tests indicating that many general, qualitative trends in blend miscibility are unchanged when the constraints of high pressure and high molecular weights are lifted (apart, of course, for the pressure dependence of the phase behavior and for the occurrence of phase diagrams with both UCST and LCST that can be described[7] with the full LCT).

The free energy of mixing Δf^{mix} for a binary polymer blend is given in the SLCT by[31]

$$\frac{\Delta f^{\mathrm{mix}}}{kT}=\frac{\phi}{M}\ln\phi+\frac{1-\phi}{M\lambda}\ln(1-\phi)+\phi(1-\phi)\times\left[\frac{(r_1-r_2)^2}{z^2}+\frac{\epsilon}{kT}\left(\frac{z-2}{2}-\frac{1}{z}\{p_1(1-\phi)+p_2\phi\}\right)\right], \tag{1}$$

where $\phi\equiv\phi_1=1-\phi_2$ is the volume fraction of component 1, $M\equiv M_1$ is the number of united atom groups in a single chain of blend species 1, $\lambda=M_2/M_1$ denotes the ratio of the chain site occupancy indices, $\epsilon=\epsilon_{11}+\epsilon_{22}-2\epsilon_{12}$ is the blend exchange energy, z designates the lattice coordination number, and T is the absolute temperature. The chain occupancy index M_i coincides with the polymerization index N_i only when a monomer is composed of one united atom group and occupies a single lattice site. Otherwise, when a monomer of species i extends over s_i lattice sites, M_i is given by $M_i=N_i s_i$. The first two terms on the right-hand side of Eq. (1) represent the configurational entropy, while the contribution $\phi(1-\phi)(r_1-r_2)^2/z^2$ is the noncombinatorial entropy of mixing which arises from local correlations associated with the packing constraints imposed by the monomer structures. The entropic coefficients r_i ($i=1,2$) are obtained from the respective numbers $s_i^{(\mathrm{tri})}$ and $s_i^{(\mathrm{tetr})}$ of tri- and tetrafunctional united atom groups in a single monomer of species i,

$$r_i=1+\frac{s_i^{(\mathrm{tri})}}{s_i}+3\frac{s_i^{(\mathrm{tetr})}}{s_i}. \tag{2}$$

The remaining terms in Eq. (1) are of energetic origin and involve both monomer structure dependent and independent contributions. A monomer structure dependence enters the composition dependent energetic terms through the geometrical factors p_1 and p_2. These topological parameters equal the numbers of distinct sets of three sequential bonds

traversing single monomers of species 1 and 2, respectively. Both p_1 and p_2 can be expressed in terms of $s_i^{(\mathrm{tri})}$ and $s_i^{(\mathrm{tetr})}$ for certain types of monomer structures, and representative calculations of p_i are described in Ref. 31. The monomer structure independent leading energetic contribution of $z\epsilon/(2kT)$ is merely the FH interaction term. This leading order for the interchain interaction grossly overestimates the number of nearest neighbor heterocontacts. The replacement of the factor of z in the FH approximation $z\epsilon/(2kT)$ by $(z-2)$ is consistent with the argument of Guggenheim[46] that each interior unit in a linear chain is linked (by chemical bonds) to the nearest neighbor units. Consequently, these two neighboring sites (using the language of the lattice model) are unavailable for occupancy by units belonging to other chains. Beyond the application of the high molecular weight, high pressure, high temperature, fully flexible polymer chain limit, Eq. (1) has been obtained by a truncation through second order of the expansion in $1/z$ that describes nonrandom mixing arising from packing of structured monomers. The ϵ^2 term, given in Ref. 31, is omitted as small and numerically irrelevant for the binary blends considered.

A. Location of critical point

The incompressible limit SANS χ parameter is defined in terms of the free energy Δf^{mix},

$$\frac{\partial^2(\Delta f^{\mathrm{mix}}/kT)}{\partial\phi^2}=\frac{1}{M\phi}+\frac{1}{M\lambda(1-\phi)}-2\chi, \tag{3}$$

where the χ parameter is expressed as an interaction parameter between united atom groups.[31,13] Evaluating the derivative in Eq. (3) converts χ into the simple polynomial,

$$\chi=a+(b+c\phi)/T, \tag{4}$$

with

$$a\equiv(r_1-r_2)^2/z^2, \tag{5}$$

being[47] the temperature independent portion of χ and with the coefficients

$$b\equiv(\epsilon/k)[(z-2)/2+(1/z)(-2p_1+p_2)]$$

and

$$c\equiv(\epsilon/k)(3/z)(p_1-p_2). \tag{6}$$

As shown below, the constants b and c exert a large influence on T dependence of χ and the shape of the phase boundary. Equations (4) and (5) provide a simple interpretation of the temperature independent portion of χ as arising from different monomer structures of the two blend components.[48] When both blend components have monomers with the same structures, a and c both *vanish* identically and the classical FH theory is recovered.[49]

The critical composition ϕ_c is determined from the vanishing of the third derivative of the free energy Δf^{mix},

$$\left.\frac{\partial^3\Delta f^{\mathrm{mix}}}{\partial\phi^3}\right|_{\phi=\phi_c}=0, \tag{7}$$

which, in turn, when applied to Eq. (1), yields the following expression:

$$-2ac\phi_c^2(1-\phi_c)^2+\frac{1}{M\lambda}[2c(\lambda-1)\phi_c^3+\{b(\lambda-1)-c(4\lambda-1)\}\phi_c^2+2(c-b)\lambda\phi_c+b\lambda]=0. \tag{8}$$

Notice that when both of the non-FH terms a and c are nonzero, the $M\to\infty$ limit leads to a highly asymmetric phase diagram with $\phi_c\to 0$ or 1.

The critical temperature T_c is obtained by solving the stability condition,

$$\frac{1}{M\phi}+\frac{1}{M\lambda(1-\phi)}-2\chi=0 \tag{9}$$

evaluated at the critical composition (volume fraction) $\phi=\phi_c$ determined by Eq. (8). This leads to the simple expression for the critical temperature,

$$T_c=\frac{2(b+c\phi_c)}{\frac{1}{M\phi_c}+\frac{1}{M\lambda(1-\phi_c)}-2a}. \tag{10}$$

The largest contribution to the shift of T_c from its FH value $T_c^{(\mathrm{FH})}$ is due to the parameter a. An increase of a generally leads to decreased blend miscibility.

B. Theta temperatures

In analogy to polymer solutions where the theta temperature T_θ is identified as an essential reference temperature,[1,3,42] T_θ can also be defined (and measured) for dilute polymer blends. Since either component of a binary blend can be the dilute species, there are *two* osmotic virial expansions and two osmotic pressures, say Π_1 and Π_2, where the subscripts 1 and 2 denote the majority species. These virial series are readily generated from Eq. (1) by evaluating the chemical potentials μ_i of species i $(i=1,2)$ and by expanding the logarithmic term about the vanishing volume fraction limits ($\phi_1\approx 0$ or $\phi_2\approx 0$),

$$\frac{\Pi_1 v_{\mathrm{cell}}}{kT}=-\frac{\mu_1}{kT}=A_1^{(1)}\phi_2+A_2^{(1)}\phi_2^2+A_3^{(1)}\phi_2^3+\cdots,\qquad \phi_2\approx 0, \tag{11}$$

and

$$\frac{\Pi_2 v_{\mathrm{cell}}}{kT}=-\frac{\mu_2}{kT}=A_1^{(2)}\phi_1+A_2^{(2)}\phi_1^2+A_3^{(2)}\phi_1^3+\cdots,\qquad \phi_1\approx 0, \tag{12}$$

where the volume v_{cell} is the average united atom group volume (the volume associated with a single lattice site) and where $A_1^{(i)}$, $A_2^{(i)}$, and $A_3^{(i)}$ are the first, second and third virial coefficients, respectively, given by

$$A_1^{(1)}=1/\lambda,\quad A_1^{(2)}=\lambda, \tag{13}$$

$$A_2^{(1)}=\frac{1}{2}-\left(a+\frac{b+c}{T}\right)M_1, \tag{14}$$

$$A_2^{(2)}=\frac{1}{2}-\left(a+\frac{b}{T}\right)M_2, \tag{15}$$

$$A_3^{(1)}=\frac{1}{3}+\frac{2}{3}\frac{c}{T}M_1, \quad A_3^{(2)}=\frac{1}{3}-\frac{2}{3}\frac{c}{T}M_2, \tag{16}$$

with a, b, and c defined by Eqs. (5) and (6). (Note that the third virial coefficient may be negative, while the second is positive.) The virial coefficients are related to the interaction parameter χ by

$$A_2^{(1)}=1/2-\chi(\phi=1)M_1, \tag{17}$$

$$A_2^{(2)}=1/2-\chi(\phi=0)M_2, \tag{18}$$

and

$$\chi=\frac{1}{M_1}\left[-\left(A_2^{(1)}-\frac{1}{2}\right)-\frac{3}{2}(1-\phi)\left(A_3^{(1)}-\frac{1}{3}\right)\right]$$
$$=\frac{1}{M_2}\left[-\left(A_2^{(2)}-\frac{1}{2}\right)-\frac{3}{2}\phi\left(A_3^{(2)}-\frac{1}{3}\right)\right], \tag{19}$$

which establishes a connection between χ and the fundamental, model-independent fluid mixture properties $[A_2^{(i)},A_3^{(i)}]$. Equations (14) and (15) imply that each binary blend has two theta temperatures,

$$T_\theta^{(1)}=\frac{2(b+c)M_1}{1-2aM_1}, \tag{20}$$

and

$$T_\theta^{(2)}=\frac{2bM_2}{1-2aM_2}. \tag{21}$$

The temperatures $T_\theta^{(1)}$ and $T_\theta^{(2)}$ tend to be near each other for ''symmetric'' blends ($\lambda=1$) since $|c/b|$ is normally small.

C. Correlation length and size of the critical region

The static correlation length ξ is another characteristic property of polymer blends which is expected to be strongly influenced by monomer shape and size asymmetries. Within mean field theory, the correlation length ξ is connected with the blend susceptibility $\omega=1/[\partial^2(f^{\rm mix}/kT)/\partial\phi^2]$ through the general relation,

$$\xi=\sqrt{d_o\omega}, \tag{22}$$

where d_o is the square gradient coefficient. The coefficient d_o can be estimated within the incompressible blend random phase approximation (RPA) (Ref. 3) in terms of the critical composition ϕ_c and the monomer Kuhn lengths l_1 and l_2,

$$d_o=\frac{1}{18}\left[\frac{l_1^2}{s_1\phi_c}+\frac{l_2^2}{s_2(1-\phi_c)}\right]. \tag{23}$$

Equations (22) and (23) enable calculating the correlation length amplitude ξ_o at the critical composition through the relation $\xi\equiv\xi_o|(T-T_c)/T|^{-1/2}$. After some algebra, ξ_o can be expressed as

$$\xi_o=\left(\frac{d_oT_c}{2|b+c\phi_c|}\right)^{1/2}. \tag{24}$$

The RPA theory assumes that blending introduces no changes in the polymer dimensions and that the chains are ideal.[3] This assumption for dilute blends is most suitable near the theta point which can be far removed from the critical point, but may be inadequate for dilute blends far from the theta point where a more sophisticated description may be required. Within the RPA approximation, ξ_o is *independent* of T. We note that the mean field sum rule $\xi^2\sim S(0)$ [$S(0)$ is the structure factor in the long wavelength limit and is proportional to the osmotic compressibility and the susceptibility ω] implies that ξ_o also controls the amplitude of composition fluctuations.[50]

Finally, the monomer shape and size asymmetry influences the ranges of T over which mean field and Ising-type critical behaviors are observed. These T ranges are expressed in terms of the Ginzburg number Gi which provides a rough estimate of the magnitude of the reduced temperature $\tau\equiv(T-T_c)/T$ at which the crossover from mean-field to Ising-type behaviors occurs. Dudowicz *et al.*[50] have introduced more refined criterion for specifying the three different regimes. Mean field theory holds for $\tau\geqslant 10{\rm Gi}$, while the Ising critical behavior corresponds to $\tau\leqslant{\rm Gi}/10$. The range ${\rm Gi}/10<\tau<10{\rm Gi}$ describes a crossover regime with $\tau\approx{\rm Gi}$ in the middle of this range. For an incompressible blend, Gi is given by[50]

$${\rm Gi}=\frac{v_{\rm cell}^2[M^{-1}\phi_c^{-3}+(M\lambda)^{-1}(1-\phi_c)^{-3}]^2}{64\pi^2|M^{-1}\phi_c^{-1}+(M\lambda)^{-1}(1-\phi_c)^{-1}-2a|d_o^3}, \tag{25}$$

with a and d_o defined by Eqs. (5) and (23), respectively.[51]

IV. CLASSES OF POLYMER BLEND MISCIBILITY

A. The M dependence of ϕ_c and T_c

The simplified LCT predicts that binary polymer blends yield four distinct classes of critical behavior. This classification is based on the analysis of Eqs. (8) and (10) which enable the evaluation of the critical parameters (ϕ_c and T_c) for eight potential types of blends that are characterized by (i) the sign of the exchange energy $\epsilon=\epsilon_{11}+\epsilon_{22}-2\epsilon_{12}$ and (ii) the degree of structural asymmetry between the monomers (i.e., whether or not a and c are nonzero). Monomer asymmetry leads to a nonvanishing ''entropic'' χ term $a\sim(r_1-r_2)^2$ and produces asymmetry in the phase diagram within the SLCT when the coefficient $c\sim(p_1-p_2)$ is nonzero.

The eight potential types of blend phase behavior arise because b may have two possible signs and because a and c may each be either zero or nonzero. Generally, the theory predicts that a is always positive, while b and c can be positive or negative. (Note, however, that the sign of c is reversed upon the label interchange $1\leftrightarrow 2$ between the two blend components.) Although experiments indicate that a for some random copolymer blends can be negative,[52] the classes of critical behavior for $a<0$ are not considered here as they do not emerge from the SLCT.

In addition to different monomer structures, blend components usually have different molecular weights. The latter difference introduces an additional source of asymmetry that is quantified in the LCT by the chain site occupancy index ratio $\lambda=M_2/M_1$, which is the natural extension of the polymerization index ratio λ_N in FH theory and which accounts

TABLE I. Classes of critical behavior for binary polymer blends as predicted by the LCT in the high pressure, high molecular weight limit.[a]

	a	b	c	M,λ		ϕ_c	T_c	Gi	$\frac{T_\theta^{(1)}-T_c}{T_c}$	$\frac{T_\theta^{(2)}-T_c}{T_c}$	ξ_o
I	$a=0$	$b>0$	$c=0$		UCST	$\frac{\sqrt{\lambda}}{1+\sqrt{\lambda}}$	$2blM$	$\sim M^{-1}$	$\frac{1+2\sqrt{\lambda}}{\lambda}$	$\lambda+2\sqrt{\lambda}$	$\sim M^{1/2}$
				$\lambda\to 0$[b]	UCST	$\sim\sqrt{\lambda}$	$2b$	$\sim M^{-1/2}$	λ^{-1}	$\sqrt{\lambda}$	$\sim M^{1/4}$
	$a=0$	$b<0$	$c=0$		m						
I	$a=0$	$b>0$	$c\neq 0$		UCST	$\approx\frac{\sqrt{\lambda}}{1+\sqrt{\lambda}}$	$\approx 2b'lM$	$\sim M^{-1}$	$\approx\frac{1+2\sqrt{\lambda}}{\lambda}$	$\approx\lambda+2\sqrt{\lambda}$	$\sim M^{1/2}$
	$a=0$	$b<0$	$c\neq 0$		m						
II	$a\neq 0$	$b>0$	$c=0$								
				$M\geqslant\frac{1}{2al}$	i						
				$M<\frac{1}{2al}$	UCST	$\frac{\sqrt{\lambda}}{1+\sqrt{\lambda}}$	$\frac{2blM}{1-2alM}$	$\sim\frac{M^{-1}}{1-2alM}$	$\frac{1+2\sqrt{\lambda}}{\lambda(1-2aM)}$	$\frac{\lambda+2\sqrt{\lambda}}{1-2a\lambda M}$	$\sim\left(\frac{M}{1-2alM}\right)^{1/2}$
II	$a\neq 0$	$b>0$	$c\neq 0$								
				$M\geqslant\frac{1}{2al}$	i						
				$M<\frac{1}{2al}$	UCST	$\approx\frac{\sqrt{\lambda}}{1+\sqrt{\lambda}}$	$\approx\frac{2b'lM}{1-2alM}$	$\sim\frac{M^{-1}}{1-2alM}$	$\approx\frac{1+2\sqrt{\lambda}}{\lambda(1-2aM)}$	$\approx\frac{\lambda+2\sqrt{\lambda}}{1-2a\lambda M}$	$\sim\left(\frac{M}{1-2alM}\right)^{1/2}$
III	$a\neq 0$	$b<0$	$c=0$								
				$M\leqslant\frac{1}{2al}$	m						
				$M>\frac{1}{2al}$	LCST	$\frac{\sqrt{\lambda}}{1+\sqrt{\lambda}}$	$\frac{2blM}{1-2alM}$	$\sim\frac{M^{-1}}{2alM-1}$	$\frac{1+2\sqrt{\lambda}}{\lambda(1-2aM)}$[c]	$\frac{\lambda+2\sqrt{\lambda}}{1-2a\lambda M}$[d]	$\sim\left(\frac{M}{2alM-1}\right)^{1/2}$
				$M\to\infty$	LCST	$\frac{\sqrt{\lambda}}{1+\sqrt{\lambda}}$	$\lvert b\rvert/a$	$\sim M^{-2}$	$\sim M^{-1}$	$\sim M^{-1}$	const[e]
IV	$a\neq 0$	$b<0$	$c\neq 0$								
				$M\leqslant\frac{1}{2al}$	m						
				$M>\frac{1}{2al}$	LCST	na	na	na	na	na	na
			$c<0$	$M\to\infty$	LCST	$\sim M^{-1/2}$	$\lvert b\rvert/a$	$\sim M^{-1/2}$	c/b	$\sim M^{-1/2}$	$\sim M^{1/4}$
			$c>0$	$M\to\infty$	LCST	$1-O\left(\frac{1}{M^{1/2}}\right)$	$\frac{\lvert b-c\rvert}{a}$	$\sim M^{-1/2}$	$\sim M^{-1/2}$	$\frac{c}{\lvert b-c\rvert}$	$\sim M^{1/4}$

[a] $l\equiv\lambda/(1+\sqrt{\lambda})^2$, $\lambda\equiv M_2/M_1$, $M\equiv M_1$, $b'\equiv b+c\sqrt{l}$, m and i denote complete miscibility and immiscibility, respectively, and na indicates the nonexistence of a physically meaningful solution.
[b] For all other cases considered, $0<\lambda<\infty$.
[c] A positive $T_\theta^{(1)}$ implies the condition $M>(2a)^{-1}$ which is a stronger constraint than $M>(2al)^{-1}$.
[d] A positive $T_\theta^{(2)}$ implies the condition $M>(2a\lambda)^{-1}$ which is a stronger constraint than $M>(2al)^{-1}$.
[e] The constant is a function of a, λ, the Kuhn lengths l_1 and l_2, and numbers (s_1, s_2) of united atom groups in the single monomers of components 1 and 2.

for different monomer sizes (e.g., volumes). The limit $\lambda\to 0$ describes a polymer solution with component 1 being the high molecular mass polymer, as mentioned in the Introduction. It is also worth mentioning that because the SLCT is formulated in the high molecular weight limit,[31] the $\lambda\approx 0$ limit corresponds to $M_1, M_2\gg 1$ and $M_1\gg M_2$. Generally, the treatment of polymer solutions must retain $1/M_2$ contributions that are neglected in Eq. (1) or, when $M_2=1$, must use the free energy expression for one component polymer systems that differs considerably[10,53] from the expression obtained from Eq. (1) by setting $r_2=p_2=0$.

The main characteristics of these four distinct classes of critical behavior are summarized in Table I along with a specification of which of the eight classes are predicted to be completely miscible or immiscible. Class I ($a=0, c=0, b>0$) yields phase diagrams similar to FH theory[1,3] and is characterized by a UCST phase separation in which the critical temperature T_c is proportional to M ($M\equiv M_1$) and in which the critical composition ϕ_c is insensitive to M, but depends only on the ratio λ. The case of $\lambda=1$ corresponds to a symmetric blend ($M_1=M_2$) and leads to $\phi_c=1/2$.

The presence of a nonzero c (for $a=0$, $b>0$) shifts the critical composition from the FH case of $\phi_c=\lambda/(1+\sqrt{\lambda})$, while the critical temperature is slightly altered as $T_c\approx 2b'M\lambda/(1+\sqrt{\lambda})^2$, where $b'=b+c\sqrt{\lambda}/(1+\sqrt{\lambda})$. The scaling $T_c\sim M$ remains, as well as the independence of ϕ_c on M. Consequently, we still designate this pattern of phase

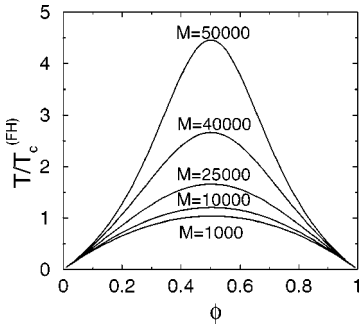

FIG. 2. The SLCT spinodal curves computed for a series of monodisperse PH1/PEP blends with varying molecular weights. Both blend components are assumed to have identical numbers of united atom groups $M_1=M_2=M$ ($\lambda=1$) in individual chains, and M values are indicated in the figure. The volume fraction $\phi\equiv\phi_1$ refers to component 1, which is P1H (in Figs. 2–4). The spinodal temperature is normalized by the critical temperature $T_c^{(FH)}$ [evaluated from Eq. (10) by setting $a=c=0$].

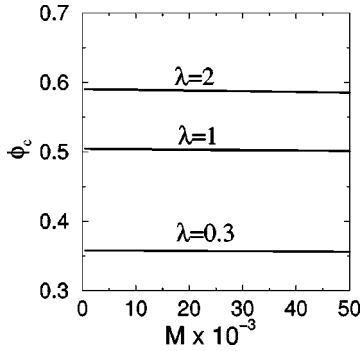

FIG. 4. The critical composition ϕ_c of monodisperse PH1/PEP blends as a function of the number of united atom groups $M\equiv M_1$ in a PH1 chain for three fixed ratios $\lambda=M_2/M_1$ as indicated in the figure. For all values of λ, ϕ_c is practically insensitive to M, in agreement with FH theory predictions.

behavior as FH type or class I, in spite of the presence of some small quantitative changes in T_c and ϕ_c.

The remaining three classes exhibit *qualitative departures* from FH behavior. Class II ($a\neq0,c=0,b>0$) also yields a UCST behavior, but with a stronger dependence of T_c on M than linear (see Table I). This stronger dependence evidently stems from the presence of a nonzero a in the denominator of Eq. (10). On the other hand, the critical composition remains identical to ϕ_c for the FH class. The occurrence of a UCST phase diagram is limited, however, to values of M smaller than the "critical" value $M_{\text{crit}}=(1+\sqrt{\lambda})^2/(2a\lambda)$, where T_c diverges. [The solution for T_c in Eq. (10) ceases to be physical for M larger than M_{crit}.] Again, the presence of nonzero c only induces quantitative shifts in T_c and ϕ_c relative to the T_c and ϕ_c for the $c=0$ case. The scaling of T_c with M and the insensitivity of ϕ_c to M remain as when $c=0$. The FH relation[1,3] $\phi_c=\sqrt{\lambda}/(1+\sqrt{\lambda})$ holds well when $b\gg c$ since this condition corresponds to a limit of small structural asymmetry.

Class III ($a\neq0,c=0,b<0$) is our first example producing LCST behavior and dramatic departures from the FH pattern of blend miscibility. The critical temperature T_c in the $M\to\infty$ limit no longer scales with M, but instead approaches the *constant* $|b|/a$. The critical composition ϕ_c still equals $\sqrt{\lambda}/(1+\sqrt{\lambda})$ due to the fact that structural asymmetry no longer affects ϕ_c when $c=0$. Class IV ($a\neq0,c\neq0,b<0$) also yields LCST phase diagrams, but differs from class III in some aspects. First, the critical composition ϕ_c depends strongly on M, as can be seen from the two large M asymptotic limiting solutions of Eq. (8),

$$\phi_c=\left(\sqrt{\frac{b}{2ac}}\right)\frac{1}{M^{1/2}}+\left(\frac{1}{2a}\right)\frac{1}{M}+\left(\frac{-b^2+c^2\lambda+bc}{4\lambda\sqrt{2ba^3c^3}}\right)\frac{1}{M^{3/2}}+\cdots,\quad c<0 \tag{26}$$

and

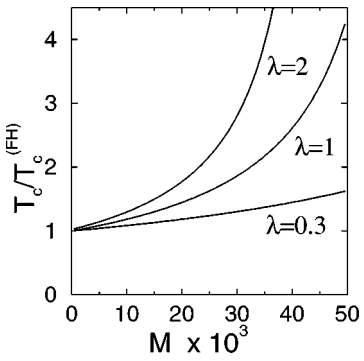

FIG. 3. The critical temperature T_c of monodisperse PH1/PEP blends as a function of the number of united atom groups $M\equiv M_1$ in a PH1 chain for three fixed ratios $\lambda=M_2/M_1$ as indicated in the figure. Component 1 is PH1, and M is a proportional to the molecular weight of PH1. The normalization of T_c by $T_c^{(FH)}$ provides a convenient visualization of departures of T_c from FH theory where $T_c/T_c^{(FH)}$ is independent of M. The faster than linear dependence of T_c on M in three curves represents the SLCT predictions for the class II critical behavior.

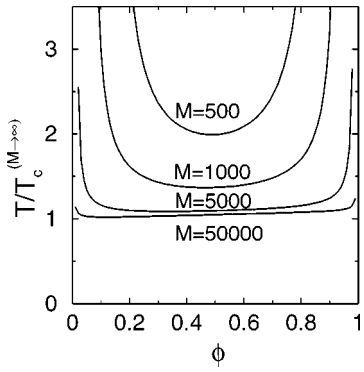

FIG. 5. The SLCT spinodal curves computed for a series of monodisperse PIB/PEP blends with varying molecular weights. Both blend components are assumed to have identical numbers of united atom groups $M_1=M_2=M$ ($\lambda=1$) in individual chains, and the M values are indicated in the figure. The volume fraction $\phi=\phi_1$ refers to component 1 which is PIB (in Figs. 5–7). The spinodal temperature is normalized by the critical temperature $T_c^{(M\to\infty)}$ corresponding to the $M\to\infty$ limit. The critical behavior of PIB/PEP blends (see Figs. 6 and 7) is designated as class IV.

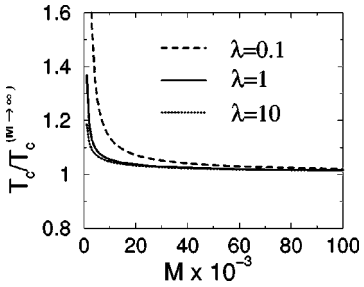

FIG. 6. The critical temperature T_c of monodisperse PIB/PEP blends as a function of number of united atom groups $M \equiv M_1$ in a PIB chain for three fixed ratios $\lambda = M_2/M_1$ as indicated in the figure. The critical temperature T_c is normalized by the critical temperature $T_c^{(M\to\infty)}$ in the $M\to\infty$ limit. As M grows, the ratio $T_c/T_c^{(M\to\infty)}$ slowly approaches unity.

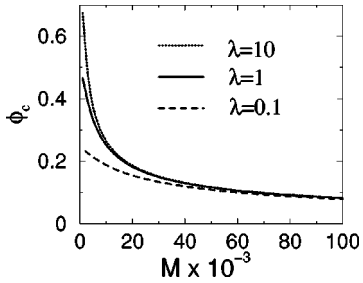

FIG. 7. The critical composition ϕ_c of monodisperse PIB/PEP blends as a function of number of united atom groups $M \equiv M_1$ in a PIB chain for three fixed ratios $\lambda = M_2/M_1$ as indicated in the figure. For large M, ϕ_c ceases to depend on λ and slowly approaches zero. The exchange energy ϵ has been taken as $\epsilon/k = -1$ K (Ref. 31).

$$\phi_c = 1 - \left(\sqrt{\frac{|b-c|}{2ac\lambda}} \right) \frac{1}{M^{1/2}} - \left(\frac{1}{2a\lambda} \right) \frac{1}{M} - \left(\frac{-b^2\lambda - c^2(2\lambda-1) - 3bc\lambda}{4\sqrt{2|b-c|a^3c^3\lambda^3}} \right) \frac{1}{M^{3/2}} - \cdots, \quad c > 0. \tag{27}$$

Secondly, in the $M\to\infty$ limit, the critical temperature T_c approaches different limits depending on the sign of c,

$$T_c = \left(\frac{|b|}{a} \right) + \left(\sqrt{\frac{2bc}{a^3}} \right) \frac{1}{M^{1/2}} + \left(\frac{|b| - 2c\lambda}{2a^2\lambda} \right) \frac{1}{M} + \left(-\frac{1}{2a^2\lambda} \left[\sqrt{\frac{b}{2ac}}(b+c) + \sqrt{\frac{c}{2ab}}(2b + c\lambda) \right] \right) \frac{1}{M^{3/2}} + \cdots, \quad c < 0, \tag{28}$$

while for positive c,

$$T_c = \left(\frac{|b-c|}{a} \right) + \left(\sqrt{\frac{2|b-c|c}{a^3\lambda}} \right) \frac{1}{M^{1/2}} + \left(\frac{|b-c|\lambda + 2c}{2a^2\lambda} \right) \frac{1}{M} + \left(-\frac{1}{2a^2\lambda} \left[\sqrt{\frac{|b-c|}{2ac\lambda}} b\lambda + \sqrt{\frac{c}{2a|b-c|\lambda}}(2b\lambda + 2c\lambda - c) \right] \right) \frac{1}{M^{3/2}} + \cdots, \quad c > 0. \tag{29}$$

Notice that a similar type of scaling for the critical parameters ($\phi_c \sim M^{-1/2}, T_c \to$ const) emerges from the SLCT for polymer solutions exhibiting an upper critical phase separation temperature (see Table I).

The two main non-FH classes of critical behavior, designated as classes II and IV, are also described graphically to better illustrate their characteristics. Figure 2 depicts the spinodal curves computed for a series of poly(hexene-1)/poly(ethylylene propylene) (PH1/PEP) blends which are typical UCST polyolefin mixtures that phase separate upon cooling.[54] For simplicity, both blend species are assumed to have identical numbers of united atom groups $M_1 = M_2 = M$ ($\lambda = 1$) in individual chains, and the different curves correspond to different values of M, as indicated in the figure. (The molar mass in amu is obtained by multiplying M by a factor of 14.) The spinodal temperature is normalized by the FH critical temperature $T_c^{(\mathrm{FH})} = 2bM\lambda/(1+\sqrt{\lambda})^2$ in order to eliminate the influence of the exchange energy on the phase boundary. This particular choice of the PH1/PEP system has been made because of its rather small value of $a = (1/z^2)(r_1 - r_2)^2 = (1/36)(7/6 - 6/5)^2 = 3.09 \times 10^{-5}$ which, in turn, implies a relatively high $M_{\mathrm{crit}} = (1+\sqrt{\lambda})^2/(2a\lambda) \approx 6 \times 10^4$ and a wide range of M over which physically realistic computed critical temperatures T_c are found. The critical temperature T_c [normalized by $T_c^{(\mathrm{FH})}$] is plotted against M in Fig. 3 for PH1/PEP blends. Deviations of the ratio $T_c/T_c^{(\mathrm{FH})}$ from unity provide quantitative measures of departures of T_c from FH theory, and some deviations can evidently be quite large. Figure 3 also shows the variation of the critical temperature T_c with λ. The already nontrivial differences between T_c and $T_c^{(\mathrm{FH})}$ for $\lambda = 1$ become even more profound for $\lambda > 1$. As mentioned earlier, the critical composition ϕ_c is insensitive to M, even when $c \neq 0$. This trend is

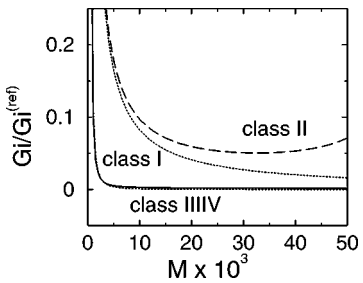

FIG. 8. The Ginzburg number Gi for "symmetric" blends ($\lambda = 1; M_1 = M_2 = M$) computed for different classes of blend miscibility as a function of the number of united atom groups M. The normalization of Gi by $\mathrm{Gi}^{(\mathrm{ref})} = 0.01$ (a typical Gi value for small molecule mixtures) provides a convenient visualization of the differences between classes I–IV. Classes II and IV are represented by PH1/PEP and PIB/PEP blends, respectively. The example for class I blends ($a = c = 0, b > 0$) is derived by choosing b as identical to b for class II, while the example for class III blends ($a \neq 0, b > 0, c = 0$) is generated by taking a and b equal to those for the PIB/PEP mixture. The exchange energies ϵ for PH1/PEP and PIB/PEP blends are taken as $\epsilon/k = 0.01$ K and $\epsilon/k = -1$ K, respectvely (Ref. 31).

evident from Fig. 4 which presents ϕ_c as a function of M for a few values of λ.

The class IV critical behavior is illustrated by specializing to the poly(isobutylene)/poly(ethylene propylene) (PIB/PEP) blend which is an example of a polyolefin blend that separates upon heating.[29] The PIB/PEP blend is described within the LCT by a negative b, a rather large entropic contribution a to χ ($a=4.82\times10^{-3}$), and by a negative c ($|c|\ll|b|$).[31] The phase boundaries (spinodals) computed for this system for various values of M and for the special case of $\lambda=1$ are presented in Fig. 5. We normalize the spinodal temperature by the critical temperature $T_c^{(M\to\infty)}$ in the $M\to\infty$ limit to remove the dependence on ϵ. An increase of M leads to a decreased miscibility, as expected, and to flatter phase boundaries, a typical feature observed[29] for binary blends of PIB with several other polyolefins (see Sec. VI). The variations of the critical temperature and critical composition with M are presented in Figs. 6 and 7, respectively, which also describe cases with $\lambda\neq1$. The critical temperature T_c [normalized by $T_c^{(M\to\infty)}$] slowly converges to unity as M grows, and T_c depends on λ only in the region of small M. A similar trend is exhibited by ϕ_c, which slowly approaches zero with the $\sim M^{-1/2}$ scaling of Table I and which ceases to depend on λ for large M as in polymer solutions. (The M-dependence of ϕ_c and T_c is illustrated for classes I–IV in our previous communication.[32]) The computed insensitivity of T_c to M in Fig. 6 accords with the experimental observation of Krishnamoorti *et al.*[29] for PIB/PEP blends. Equations (26)–(29) provide very good approximations to both T_c and ϕ_c of PIB/PEP for $M>10^4$.

B. Width of critical region

Monomer shape and size asymmetry can greatly influence the width of the critical regime and its measure, the Ginzburg number Gi. For FH type (class I) blends, the scaling[3,35,36] $\mathrm{Gi}\sim M^{-1}$ indicates a strong decrease of the critical region width with increasing M. However, the magnitude of Gi can be larger for class II blends which exhibit a shallow *minimum* in Gi as a function of M (see Fig. 8). A typical magnitude for the minimum value of Gi for class II blends is about 0.001, which is small relative to typical values of Gi for small molecule mixtures ($\mathrm{Gi}\approx0.01$).[55] The Gi for class III blends decreases even more rapidly than Gi for class I, while the dependence of Gi on M for class IV ($\mathrm{Gi}\sim M^{-1/2}$) is weaker than for class I, resembling the Gi scaling for UCST polymer solutions (see Table I).[37] Apparently, the examples of class II–IV blends indicate large departures from the $\mathrm{Gi}\sim M^{-1}$ scaling of the FH model (see Fig. 8), but there is nonetheless a general tendency for Gi to become small for large M.

C. Correlation length amplitude ξ_o

Inspection of Table I indicates that the M dependence of the correlation length amplitude ξ_o provides a particularly good indication of blend class type. For symmetric ($\lambda=1$) class I blends, ξ_o scales as the chain average radius of gyration $\xi_o\sim M^{1/2}$, a scaling that is a well known result of RPA theory[3] for polymer blends. The M dependence of ξ_o is enhanced over FH scaling for class II blends, while it is diminished for class III blends. Finally, ξ_o of class IV blends exhibits a weak M dependence ($\xi_o\sim M^{1/4}$), which coincides with the scaling behavior of ξ_o for polymer solutions (class I, $\lambda\approx0, M\to\infty$) predicted theoretically[41] and observed experimentally[56] outside the critical regime where mean-field theory is applicable. It is, thus, apparent that the scale of composition fluctuations in blends can be much smaller than predicted by FH/RPA theory.

These dramatic departures in the M dependence of ξ_o from the predictions of FH theory are easily understood from Eq. (24) which shows that ξ_o is controlled predominantly by T_c and ϕ_c. The constancy of T_c in the $M\to\infty$ limit for classes III and IV leads, in conjunction with Eqs. (23) and (24), to the scaling $\xi_o\sim\phi_c^{-1/2}$, with the proportionality constant depending on molecular parameters (l_1,l_2,s_1,s_2,b,c). The insensitivity of ϕ_c to M for class III implies that ξ_o is independent of M for large M, while the scaling $\phi_c\sim M^{-1/2}$ in the $M\to\infty$ limit for class IV yields the scaling $\xi_o\sim M^{1/4}$. We expect that the power law $\xi_o\sim\phi_c^{-1/2}$ also applies to branched polymer solutions for which T_c becomes constant[57] when polymer molecular mass is large. Notably, this interelation between ξ_o and ϕ_c also appears to hold in the non-classical critical regime of polymer solutions where[56] $\phi_c\sim M^{-0.385}$ and $\xi_o\sim M^{0.195}$.

D. Gap between theta temperature and critical temperature

The ratios of the blend theta temperatures $T_\theta^{(1)}$ and $T_\theta^{(2)}$ to the critical temperature T_c for phase separation also provide valuable information about the blend class type. We define the reduced temperature gap δT_θ between the theta temperature and T_c as

$$\delta T_\theta^{(i)}=(T_\theta^{(i)}-T_c)/T_c, \tag{30}$$

and analyze how this quantity varies for the various classes. For case I (FH class), Table I indicates that $\delta T_\theta^{(1)}$ and $\delta T_\theta^{(2)}$ approach zero for large molecular mass asymmetry ($\lambda\to\infty$ and $\lambda\to0$, respectively), but both $\delta T_\theta^{(1)}$ and $\delta T_\theta^{(2)}$ become large for symmetric blends [$\delta T_\theta^{(1)}=\delta T_\theta^{(2)}=3$ for $\lambda=1$ or, equivalently, $T_\theta^{(1)}/T_c=T_\theta^{(2)}/T_c=4$].[58] When T_c is near room temperature (≈300 K), the condition $\delta T_\theta^{(i)}=3$ would imply a theta temperature of about 1200 K. Of course, most polymers would thermally degrade at such temperatures, so that this result does not appear very interesting. Indeed the study of theta temperatures in blends might be dismissed altogether based solely on this result.

We contrast $\delta T_\theta^{(i)}$ ($i=1,2$) for the FH class I to those for class IV blends. Table I illustrates that in the $M\to\infty$ limit, one of the class IV theta temperatures coincides with T_c, while the other is independent of molecular mass asymmetry (λ). Thus, it should be easy to observe a theta point(s) for class IV blends,[59,60] as well as the same type of associated chain swelling and contraction with varying "solvent quality" in dilute blends as found in dilute polymer solutions.[61] A unique behavior of $\delta T_\theta^{(i)}$ is obtained in class III where both $\delta T_\theta^{(1)}$ and $\delta T_\theta^{(2)}$ approach zero as $M\to\infty$, which implies that the limiting theta temperatures coincide with T_c. Class II

exhibits more complex behavior since $\delta T_\theta^{(1)}$ and $\delta T_\theta^{(2)}$ both depend strongly on λ and M. In summary, the observation of one or two theta temperatures in real (dilute) blends should be possible in many cases, providing direct evidence of non-FH classes of blend miscibility. Note that the $\delta T_\theta^{(i)}$ are negative or zero for LCST type blends, and the two theta temperatures $T_\theta^{(1)}$ and $T_\theta^{(2)}$ are close to each other for symmetric blends ($\lambda=1$). The M-dependence of $\delta T_\theta^{(1)}$ for symmetric blends of classes I-IV is illustrated in our previous communication.[32]

V. EXPERIMENTAL SUPPORT FOR NEW CLASSES OF POLYMER BLEND MISCIBILITY

As mentioned earlier, a linear scaling of T_c with M has been obtained from SANS experiments for symmetric ($N_1=N_2$) isotopic polyolefin blends (where molecular monomer structures are almost identical) and has been confirmed by Monte Carlo simulations.[23,24] There are, however, several experimental observations indicating that this FH pattern of blend miscibility is not general. Perhaps, the best documented example of this nonuniversality is provided by the polystyrene/poly(vinyl methyl ether) (PS/PVME) blend. The SANS experiments by Han *et al.*[27] reveal that T_c for this system is nearly independent of M, and the phase boundary is highly asymmetric.[27,28] For two PS/PVME samples specified by approximately the same λ (λ_N) but different molecular masses (differing by a factor of 3), the experimental critical compositions $\phi_c \equiv \phi_c^{(\mathrm{PS})} \approx 0.2$ and 0.1 for these two blends depart significantly from the predictions $\phi_c^{(\mathrm{FH})} = \sqrt{\lambda_N}/(1+\sqrt{\lambda_N}) \approx 0.64$ and 0.65, respectively, of FH theory. The SLCT predicts that ϕ_c should scale as $M^{-1/2}$ for class IV, so that a factor of 3 increase in M between the two blends should thus lead to a reduction of ϕ_c by $\sqrt{3} \approx 1.7$. This prediction is consistent with the data of Han *et al.*[27] where roughly a factor of 2 reduction is observed. (PS/PVME blends are classified as type IV blends, based on fits to blend scattering data and the resulting conditions $b<0$, and $a, c \neq 0$.) Other aspects of non-FH-type critical behavior of PS/PVME blends are described in our prior studies of this system.[8,9,34] Measurements[27,62] and LCT computations[50] for PS/PVME mixtures over a limited range of M indicate a weak M-dependence of the correlation length amplitude ξ_o (typical values[63] of ξ_o are on the order of 10 Å), and the theta temperature of PS dispersed at a low concentration in PVME has been estimated[60] as $T_\theta^{(\mathrm{PVME})} = 147\,^\circ\mathrm{C}$, a value remarkably close to the critical temperature values found by Han *et al.*,[27] $T_c = 145 \pm 5\,^\circ\mathrm{C}$. A similar insensitivity of T_c to M is reported[29] for binary blends of PIB with several other polyolefins, which provide additional examples of LCST systems and class IV blends. All these measurements are consistent with the properties derived for class IV polymer blends, which strikingly resemble properties of upper critical temperature polymer solutions. As shown in Table I, the scalings of T_c, ϕ_c, Gi, $\delta T_\theta^{(i)}$ ($i=1,2$), and ξ_o with M are identical for LCST blends (class IV) and polymer solutions of class I.[64]

A similar insensitivity of T_c to M has been observed for binary blends of PIB with several other polyolefins, where it is difficult to imagine that any "specific interactions" could be responsible for the observed dramatic deviations from FH theory. (Notably, our explanation of the non-FH critical behavior for PS/PVME blends likewise does not require invoking "special interactions.") The LCST phase separation in these systems is predicted to arise within the SLCT from the competition between a negative energetic portion of the χ parameter and a sufficiently positive "entropic" part a of χ. The PIB blends exhibit a large a term due to the presence of a tetrafuctional carbon atom in the PIB monomer. The negative exchange energy ϵ (implying $b<0$) may occur because 50% of the PIB united atom groups are CH_3 groups that have larger attractive interactions (i.e., Lennard-Jones interaction parameters) than the CH_2, CH, and C united atom groups.[65] This effect produces a large self-interaction $\epsilon_{11} \equiv \epsilon_{\mathrm{PIB-PIB}}$ (relative to ϵ_{22}) and a large heterocontact interaction ϵ_{12}, leading to a negative $\epsilon = \epsilon_{11} + \epsilon_{22} - 2\epsilon_{12}$.

We contrast the scaling of T_c and other critical properties found for PS/PVME and PIB/PEP blends with those obtained by Gehlsen *et al.*[25] for an isotopic symmetric blend of poly(ethylene propylene) with its partially deuterated counterpart. As expected, this near symmetric blend exhibits scaling characteristics compatible with properties of FH class I blends, such as the inverse proportionality of χ (at the critical point) to N and the proximity of ϕ_c to 1/2.

An interesting departure from FH theory has been reported by Bates and co-workers[30] who find a *weaker* than a linear dependence of T_c on M for poly(ethylene propylene)/poly(ethylene-co-ethylethylene) (PEP/PE-PEE) mixtures which are random copolymer polyolefin blends. Notably, the weaker than linear dependence is inconsistent with the scalings predicted by the SLCT for homopolymer blends (see Table I). [The extension[66] of SLCT to copolymer systems yields χ with the same structure as in Eq. (4), but with more complicated expressions for a, b, and c.] As already mentioned, the "entropic" part a of the χ parameter is nonnegative within the SLCT theory. Experiments, on the other hand, demonstrate that some random copolymer polyolefin blends exhibit[52] a negative a. While we can not account for the negative sign of a without lifting both the incompressibility and chain flexibility assumptions of the SLCT (see below), allowing for $a<0$ in the expression $T_c = 2blM/(1-2alM)$ derived for class II UCST blends (see Table I) immediately explains the observed weaker than FH variation of T_c with M for PEP/PE-PEE blends. Since these systems phase separate upon cooling[30] and exhibit a very small (almost vanishing) χ parameter,[30] a negative a must compensate the positive b/T term in order to produce $\chi \approx 0$. We are unaware of other molecular mass studies of blend miscibility that could be used to test our classification of binary blend critical behavior. Stronger support for the theory requires data describing the M dependence of T_c, $T_\theta^{(i)}$ ($i=1,2$), ϕ_c, Gi, and ξ_o, and hopefully such data will be available in the future.

VI. DISCUSSION

The simplified lattice cluster theory (SLCT) predictions demonstrate that monomer structural asymmetry in polymer

blends qualitatively affects the miscibility, chain conformations, and critical properties of binary polymer blends. The theoretical analysis has been applied to eight potential types of blends characterized by the sign of the exchange energy ϵ (b), the degree of monomer structural asymmetry (a,c), and whether or not the "entropic" portion a of the χ parameter is nonzero. (When both a and c are zero, the effective interaction parameter χ reduces to a form similar to that predicted by FH theory.) In addition to structural asymmetry, the two blend components may exhibit chain length asymmetry, which is represented in the SLCT by the ratio $\lambda = M_2/M_1$ (where M_1 and M_2 are the chain site occupancy indices). The ratio λ is the natural extension of the polymerization index ratio λ_N in FH theory to account for different monomer sizes. Within these eight possible categories, we distinguish four classes of distinct critical behavior that are specified by unique scalings with $M \equiv M_1$ of the critical temperature T_c, critical composition ϕ_c, the Ginzburg number Gi, the correlation length amplitude ξ_o, as well as the distances $\delta T_\theta^{(i)} (i=1,2)$ of the theta temperatures [$T_\theta^{(1)}$ and $T_\theta^{(2)}$] for the two possible dilute blend limits from the critical temperature T_c. While both T_c and ϕ_c govern the position and shape of phase boundaries, Gi, $\delta T_\theta^{(i)}$, and ξ_o control the width of critical region, the extent of chain swelling near T_c, and the scale of composition fluctuations in the mean field regime, respectively. The correlation length amplitude also regulates the magnitude of the blend interfacial tension[67] and other important properties (scattering intensity, collective diffision coefficient, etc.). A graphical illustration of the general scalings of $T_c(M)$, $\phi_c(M)$, $\xi_o(M)$, and $\delta T_\theta(M)$ with molecular weights M is presented in Ref. 32 for these four different classes of symmetric $(M_1 = M_2 = M)$ blends, while Figs. 2–7 of the current paper describe rather specific examples of classes II and IV blends.

A. Compressibility, interaction asymmetry, and chain stiffness

Our description of four general categories of critical behavior for polymer blends is based on the simplest version of the lattice cluster theory.[31] This choice is dictated by analytical tractability and the simplicity of the SLCT which contains only a single adjustable parameter (the exchange energy ϵ). An additional argument for the use of the SLCT stems from our observations that the theory faithfully reproduces many trends predicted by more general versions of the LCT that, of necessity, require the introduction of additional parameters. The SLCT, however, exhibits some obvious limitations, and we now discuss the differences that would emerge from the use of more general LCT formulations.[6,7,50]

The assumption of the high pressure (incompressible) limit implies that all computed excess thermodynamic properties of binary homopolymer blends depend on a single energy parameter ϵ, which is a linear combination of homocontact and heterocontact van der Waals interactions. Consequently, any influence of asymmetry in polymer-polymer homocontact interactions (i.e., differences between ϵ_{11} and ϵ_{22}) on the predicted phase behavior cannot be examined within the incompressible limit. In general, compressibility magnifies nonrandom mixing effects and may even lead in some cases to a reentrant phase diagram or to a phase boundary with separate upper and lower critical temperature branches.[7,33] Obviously, blend compressibility must affect the shape of the phase boundary, especially when ϵ_{11} and ϵ_{22} are disparate.[7,68] A useful illustration of how compressibility alters the phase boundary is provided by our previous LCT calculations[50] for PS/PVME blends. The PS/PVME spinodal curves computed by the LCT are highly asymmetric and steep (see Fig. 2 of Ref. 50), in contrast to the spinodals generated by the SLCT. The computed highly asymmetric phase diagrams for the compressible PS/PVME blends arise from the presence[50] of quite different self-interactions $\epsilon_{11} \equiv \epsilon_{\mathrm{PS-PS}}$ and $\epsilon_{22} \equiv \epsilon_{\mathrm{PVME-PVME}}$ which, in turn, induce a large variation of the blend compressibility (or excess free volume) with the blend composition. The SLCT spinodals for PS/PVME blends (not shown here) are rather flat and resemble those presented in Fig. 5 for PIB/PEP mixtures. The experimental observation[29] of the insensitivity of the spinodal temperature to the composition of PIB/PEP blends can be explained by near equality between $\epsilon_{11} \equiv \epsilon_{\mathrm{PIB-PIB}}$ and $\epsilon_{22} \equiv \epsilon_{\mathrm{PEP-PEP}}$ and by the resulting constancy of the blend free volume over the whole range of blend compositions. Thus, when the blend compressibility is independent of blend composition, it may affect the magnitude of both T_c and ϕ_c, but does not introduce an extra asymmetry into phase boudaries. We also expect that compressibility should influence the dependence of the correlation length amplitude ξ_o and the Ginzburg number Gi on M. The class IV scaling for the correlation length amplitude $\xi_o \sim M^{1/4}$ compares reasonably well with the dependence of ξ_o on M estimated by the full LCT (see Fig. 17 of Ref. 50) for large M, with deviations occurring mostly in the region of small M. (ξ_o from compressible LCT calculations is nearly independent of M when M is small.[50]) Apparently, power laws for critical properties should be different in the very long and shorter chain limits, and these differences have recently been discussed in connection with the properties of polymer solutions.[69] The predicted scaling of the Ginzburg number $\mathrm{Gi} \sim M^{-1/2}$ for class IV blends from the SLCT model exhibits a more significant departure from the full LCT.[50] The discrepancies in Gi due to the neglect of compressibility effects can be as large as a factor of five for PS/PVME blends (see Fig. 8 of Ref. 50).

The limiting high pressure (incompressible), high molecular weight LCT can readily be extended to include chain semiflexibility[9] (and thereby model chain tacticity), but only at the expense of introducing "bending" energies E_b that reflect the conformational energy differences in the actual polymers.[9] This extension[31] merely renders the two basic counting indices r_i and p_i as dependent on temperature T, whereupon the a, b, and c in Eqs. (8) and (10) then become functions of T. The same Eqs. (9) and (10) still determine the spinodal curve and critical temperature, respectively, but the equations can only be solved numerically.

The full LCT for compressible systems of polymers with finite molecular weights is essential for describing the pressure dependence of phase behavior,[34] and this theory predicts the emergence of additional patterns of blend miscibility, such as phase boundaries with closed loops, with both upper

and lower critical points, or with a miscibility gap (i.e., without a critical temperature).[7,33] These compressible systems are affected by energetic asymmetries between the constituent monomers, and numerical treatments are generally required for specific systems.

It should be noted that the LCST phase diagrams emerge from the simplified LCT for incompressible systems due to the presence of an entropic χ (the a term) and a negative b (effective attractive interactions). This mechanism is quite different from the common explanation of a LCST critical behavior that attributes the occurrence of a phase separation upon heating to the increasingly disparate densities of the polymer components at elevated temperatures, thereby producing an entropic penalty to miscibility.[70] This behavior is readily understood for polymer solutions where the LCST is usually near T_c for the pure solvent.[71] However, the components in binary blends of polyolefins, for instance, have rather similar densities and coefficients of thermal expansion, thereby vitiating for these blends the compressibility mechanism that describes LCST phase behavior in polymer solutions. Compressibility effects have been excluded as the origin of the LCST critical behavior for PS/PVME blends.[28]

B. Copolymer blends and other complex systems

The limiting high pressure (incompressible), high molecular weight LCT is likewise readily extended to treat the critical properties of blends containing copolymers.[66] The evaluation of the b and c parameters for copolymer systems is somewhat more complicated because the b term depends on monomer sequence, while the magnitudes and signs of both b and c are affected by the copolymer compositions x and y and by energetic asymmetries between different monomers, a feature that could possibly yield larger ratios c/b and, hence, more asymmetric phase diagrams and shifts to Gi in classes I and II. Because of the greater computational complexity and the presence of additional adjustable parameters (i.e., more interaction energies), the study of how chain semiflexibility and the copolymer nature of the blend components affects phase behavior is deferred to the future.

It is clear, in principle, that finite size constraints, such as blend confinement to thin blend films, should lead to changes in the magnitude of a and c (while b may remain relatively unchanged) and, consequently, to different patterns of critical behavior. For instance, ξ_o should be different in polymer blends, thin blend films, blends filled with nanoparticles, or blends in nanoporous media since the presence of heterogeneities alters the influence of monomer shape and size asymmerties on the entropy of mixing. This complexity in critical properties can be expected as a general feature of mixtures containing fluid elements (molecules, membranes, micelles, etc.) with many internal degree of freedom[72] and with complex geometrical structure. A systematic study of the classes of blend miscibility is then not only important from the standpoint of rationally designing blends with improved miscibility characteristics, but should be informative about much broader classes of complex fluid mixtures, such as those occurring in biological systems.

In summary, we demonstrate that the presence of monomer structural asymmetry can profoundly affect the blend miscibility (T_c, ϕ_c), phase boundary shape (ϕ_c), chain swelling $(T_\theta^{(1)})$, the magnitude of composition fluctuations[73] (ξ_o), as well as the width of the critical region over which Ising critical behavior is observed (Gi). The FH class of blends corresponds to just one of four basic classes of blend miscibility indentified by our simplified lattice cluster theory. One of the three remaining classes (the LCST class IV) exhibits critical behavior resembling that of UCST polymer solutions. Apparently, the monomer scale asymmetry in these polymer blends plays a similar role to the molecular mass of a polymer in polymer solutions. The other two non-FH blend miscibity classes have their own unique characteristics. Class II blends exhibit a stronger dependence of T_c on M than FH-type blends, and Gi does not vanish as M becomes large. Class III blends provide another pattern of blend miscibilty: T_c is insenitive to molecular mass, but ϕ_c depends on λ in a similar fashion as for FH-type blends. The Gi is predicted to decrease more rapidly for case III than for class I, while the correlation length amplitude in class III is independent of M. These strong differences in the M dependence of blend critical properties (see Table I for a complete review) should have practical ramifications in controling blend properties. Our analysis of binary blend critical behavior also produces an important message for experimental studies. The estimation of T_c, ξ_o, and other critical properties of polymer blends often assumes the validity of the FH expression for the critical composition $\phi_c^{(\mathrm{FH})} = \sqrt{\lambda_N}/(1+\sqrt{\lambda_N})$. This assumption can lead to gross errors in estimated critical parameters $(\phi_c, T_c, \xi_o, \ldots)$, especially for LCST systems. Since the coefficients a, b, and c can be obtained from other sources than the SLCT, such as computer simulations, experiments, or PRISM theory, the classification of blend miscibility in Table I may apply more generally.

ACKNOWLEDGMENTS

This research is supported, in part, by NIH Grant No. GM56678. The authors thank M. Muthukumar and Frank Bates for stimulating discussions.

[1] P. J. Flory, *Principles of Polymer Chemistry* (Cornell University Press, Ithaca, 1953); M. L. Huggins, J. Chem. Phys. **9**, 440 (1941); P. J. Flory, *ibid.* **9**, 660 (1941); A. J. Staverman, Recl. Trav. Chim. Pays-Bas. **60**, 640 (1941).
[2] P. J. Flory, Discuss. Faraday Soc. **49**, 7 (1970).
[3] P. G. de Gennes, J. Phys. (Paris) **31**, 235 (1970); *Scaling Concepts in Polymer Physics* (Cornell University Press, Ithaca, 1979).
[4] S. C. Glotzer, Annu. Rev. Comput. Phys. **2**, 1 (1995). See references cited in this paper for further studies of the dynamics of polymer phase separation.
[5] A. M. Thayer, Chem. Eng. News **11**, 15 (1995); P. S. Subramanian and K. J. Chou, Trends Polym. Sci. **3**, 248 (1995).
[6] J. Dudowicz and K. F. Freed, Macromolecules **24**, 5076 (1991); M. G. Bawendi and K. F. Freed, J. Phys. Chem. **86**, 3720 (1987); A. M. Nemirovsky, M. G. Bawendi, and K. F. Freed, J. Chem. Phys. **87**, 7272 (1987); K. F. Freed, J. Phys. A **18**, 871 (1985).
[7] K. F. Freed and J. Dudowicz, Theor. Chim. Acta **82**, 357 (1992).
[8] J. Dudowicz and K. F. Freed, Macromolecules **24**, 5112 (1991).
[9] K. W. Foreman and K. F. Freed, Macromolecules **30**, 7279 (1997), J. Chem. Phys. **106**, 7422 (1997).
[10] K. W. Foreman and K. F. Freed, Adv. Chem. Phys. **103**, 335 (1998).
[11] R. Koningveld, L. A. Kleintjens, and E. Niels, Croat. Chem. Acta **60**, 53 (1987).
[12] K. F. Freed, J. Dudowicz, and K. W. Foreman, J. Chem. Phys. **108**, 7881

(1998); C. Delfolie, L. C. Dickinson, K. F. Freed, J. Dudowicz, and W. J. MacKnight, Macromolecules **32**, 7781 (1999); J. Dudowicz and K. F. Freed, *ibid.* **33**, 5192 (2000).
[13] J. Dudowicz and K. F. Freed, Macromolecules **33**, 9777 (2000).
[14] J. Dudowicz, M. S. Freed, and K. F. Freed, Macromolecules **24**, 5096 (1991).
[15] J. Dudowicz and K. F. Freed, Macromolecules **26**, 213 (1993).
[16] S. Jansen, D. Schwahn, K. Mortensen, and T. Springer, Macromolecules **26**, 5587 (1993); B. Hammouda and B. J. Bauer, *ibid.* **28**, 4505 (1995).
[17] T. P. Russell, T. E. Karis, Y. Gallot, and A. M. Mayers, Nature (London) **368**, 729 (1994); T. E. Karis, T. P. Russell, Y. Gallot, and A. M. Mayes, Macromolecules **28**, 1129 (1995).
[18] K. S. Schweizer and J. G. Curro, Adv. Polym. Sci. **116**, 319 (1994); K. S. Schweizer and J. G. Curro, Adv. Chem. Phys. **98**, 1 (1997).
[19] G. H. Fredrickson, A. J. Liu, and F. S. Bates, Macromolecules **27**, 2503 (1994).
[20] F. S. Bates, M. F. Schultz, J. H. Resendale, and K. Almdal, Macromolecules **25**, 5547 (1992).
[21] W. Siol, Makromol. Chem., Macromol. Symp. **44**, 47 (1991); H.-G. Braun and G. Rehage, Angew. Makromol. Chem. **131**, 107 (1985).
[22] A. Sariban and K. Binder, J. Chem. Phys. **86**, 5859 (1987); Macromolecules **21**, 711 (1988); H.-P. Deutsch and K. Binder, *ibid.* **25**, 6214 (1992).
[23] M. Müller and K. Binder, Macromolecules **28**, 1825 (1995).
[24] F. A. Escobedo and J. J. de Pablo, Macromolecules **32**, 900 (1999).
[25] M. D. Gehlsen, J. H. Rosendale, F. S. Bates, G. D. Wignall, L. Hansen, and K. Almdal, Phys. Rev. Lett. **68**, 2452 (1992).
[26] F. S. Bates, J. H. Rosendale, P. Stepanek, T. P. Lodge, P. Wiltzius, G. H. Fredrickson, and R. P. Hjelm, Phys. Rev. Lett. **65**, 1893 (1990).
[27] C. C. Han, B. J. Bauer, J. C. Clark, Y. Muroga, Y. Matsushita, M. Okaa, Q. Tran-cong, T. Chang, and I. C. Sanchez, Polymer **29**, 2002 (1988); C. C. Han, M. Okada, Y. Muroga, B. J. Bauer, and Q. Tran-cong, Polym. Eng. Sci. **26**, 1208 (1986).
[28] B. Hammouda and B. J. Bauer, Macromolecules **28**, 4505 (1995).
[29] R. Krishnamoorti, W. W. Graessley, L. J. Fetters, R. T. Garner, and D. J. Lohse, Macromolecules **28**, 1252 (1995).
[30] F. S. Bates, M. F. Schulz, and J. H. Rosendale, Macromolecules **24**, 5096 (1991); see Ref. 39 for a comparison of the Bates *et al.* data with FH theory.
[31] K. F. Freed and J. Dudowicz, Macromolecules **31**, 6681 (1998). The simplified LCT was formally called the ''pedestrian model.''
[32] J. Dudowicz, K. F. Freed, and J. F. Douglas, Phys. Rev. Lett. **88**, 095503 (2002).
[33] J. Dudowicz and K. F. Freed, Macromolecules **29**, 8960 (1996); J. Dudowicz, K. F. Freed, and J. F. Douglas, *ibid.* **28**, 2276 (1995); M. Lifschitz, J. Dudowicz, and K. F. Freed, J. Phys. Chem. **100**, 3957 (1994).
[34] J. Dudowicz and K. F. Freed, Macromolecules **28**, 6625 (1995).
[35] P. G. de Gennes, J. Phys. (France) Lett. **38**, L441 (1977); J. F. Joanny, J. Phys. A **11**, 117 (1978).
[36] K. Binder, Phys. Rev. A **29**, 341 (1984); J. Chem. Phys. **79**, 6387 (1983).
[37] R. Holyst and T. A. Vilgis, J. Chem. Phys. **99**, 4835 (1993).
[38] H.-P. Deutsch and K. Binder, J. Phys. II **3**, 1049 (1993).
[39] C. Singh and K. S. Schweizer, Macromolecules **30**, 1490 (1997); see references cited in this paper.
[40] Simulations of Mackie *et al.* [J. Chem. Phys. **102**, 1014 (1995)] indicate that the ratio $T_c(N_1\to\infty,N_2=1)/T_c(N_1=N_2=1)\approx 3.48$, whereas the theoretical analysis by Douglas and Ishinabe [Phys. Rev. E **51**, 1791 (1995)] estimates this ratio as 10/3.
[41] P. G. de Gennes, Phys. Lett. A **26**, 313 (1968).
[42] K. F. Freed, *Renormalization Theory of Macromolecules* (Wiley, New York, 1987).
[43] J. des Cloizeaux and G. Jannick, *Polymers and Solutions: Modeling and Structure* (Clarendon, Oxford, 1990).
[44] B. Duplantier, J. Phys. (France) **43**, 991 (1982).
[45] M. A. Anisimov, V. A. Agayan, and E. E. Gorodetskii, JETP Lett. **72**, 578 (2000); M. A. Anisimov, A. F. Kostko, and J. V. Sengers, Phys. Rev. E (in press).
[46] E. A. Guggenheim, Proc. R. Soc. London, Ser. A **183**, 303 (1944); **183**, 213 (1944); A. R. Miller, *Theory of Solutions of High Polymers* (Oxford University press, New York, 1948).
[47] The contribution to a of order $1/z^3$ very probably depends on ϕ.
[48] We note that Frankel and Louis [Phys. Rev. Lett. **68**, 3363 (1992); see also M. Dijkstra and D. Frenkel, *ibid.* **72**, 298 (1984); D. Frenkel, Physica A **263**, 26 (1999)] have considered an exactly solvable model involving a mixture of dissimilarly sized squares in two dimensions that gives insights into the physical origin of the ''entropic'' contribution to χ.
[49] Our united atom model implies that $a=c=0$ for isotopic blends. Experiments indicate, however, that a and c are small, but nonzero, so the use of our model is clearly approximation for such blends.
[50] J. Dudowicz, M. Lifschitz, K. F. Freed, and J. F. Douglas, J. Chem. Phys. **99**, 4804 (1993).
[51] The square gradient coefficient d_o is denoted in Ref. 50 as c_o.
[52] See, for instance, W. W. Graessley, R. Krishnamoorti, N. P. Balsara, L. J. Fetters, D. J. Lohse, D. N. Schulz, and J. A. Sissano, Macromolecules **27**, 2574 (1994); H. Jinnai, H. Hasegawa, T. Hashimoto, and C. C. Han, *ibid.* **25**, 6078 (1992).
[53] J. Dudowicz, K. F. Freed, and W. G. Madden, Macromolecules **23**, 4803 (1990).
[54] G. H. Reichart, W. W. Graessley, R. A. Register, and D. J. Lohse, Macromolecules **31**, 7886 (1998).
[55] M. A. Anisimov, S. B. Kisielev, J. V. Sengers, and S. Tang, Physica A **188**, 487 (1992); J. M. H. Levelt-Sengers and J. V. Sengers, in *Perspectives in Statistical Physics*, edited by H. J. Raveche (North–Holland, Amsterdam, 1981), Chap. 14.
[56] Y. B. Melnichenko, G. D. Wignall, and W. A. Van Hook, Europhys. Lett. **48**, 372 (1999); P. Debye, H. Coll, and D. Woermann, J. Chem. Phys. **33**, 1746 (1960).
[57] K. Kajiwara, W. Burchard, L. A. Kleintjens, and R. Koningsveld, Polym. Bull. **7**, 191 (1982).
[58] The mean field theory ratio of $T_\theta/T_c=4$ is reduced to a value of about 3 by fluctuation effects [J. F. Douglas and T. Ishinabe, Phys. Rev. E **51**, 1791 (1995)].
[59] R. M. Briber, B. J. Bauer, and B. Hammouda, J. Chem. Phys. **101**, 2592 (1994).
[60] S. Choi, X. Lin, and R. M. Briber, J. Polym. Sci. B **36**, 1 (1998).
[61] K. S. Petersen, A. D. Stein, and M. D. Fayer, Macromolecules **23**, 111 (1990); A. Sariban and K. Binder, Macromol. Chem. Phys. **189**, 2357 (1988).
[62] Y. B. Melnichenko, G. D. Wignall, and D. Schwahn (unpublished).
[63] M. Shibayama, H. Yang, R. S. Stein, and C. C. Han, Macromolecules **18**, 2179 (1985).
[64] The general limitations of the SLCT in treating polymer solutions do not hinder the derivation of the scalings for polymer solutions (class I) since both a and c are zero.
[65] M. Mondello, G. S. Grest, A. R. Garcia, and B. G. Sibernagel, J. Chem. Phys. **105**, 5208 (1996); J. I. Siepmann, M. G. Martin, C. J. Mundy, and M. L. Klein, Mol. Phys. **90**, 687 (1997); B. Smit, S. Karaboni, and J. I. Siepmann, J. Chem. Phys. **102**, 2126 (1995).
[66] J. Dudowicz and K. F. Freed, Pol. J. Chem. **75**, 527 (2001); Macromolecules **33**, 3467 (2000).
[67] J. Cahn and J. E. Hilliard, J. Chem. Phys. **28**, 258 (1958); H. Chaar, M. R. Moldover, and J. W. Schmidt, *ibid.* **85**, 418 (1986); M. R. Moldover, Phys. Rev. A **31**, 1022 (1985); B. Widom, J. Stat. Phys. **52**, 1343 (1988).
[68] H.-P. Deutsch, J. Chem. Phys. **99**, 4825 (1993).
[69] A. A. Povodyrev, M. A. Anisimov, and J. V. Sengers, Physica A **264**, 345 (1999).
[70] I. C. Sanchez and R. H. Lacombe, Macromolecules **11**, 1145 (1978); D. Patterson, *ibid.* **2**, 672 (1969); D. Patterson, G. Delmas, and T. Somcynsky, Polymer **8**, 503 (1967); J. M. Bardin and D. Patterson, *ibid.* **10**, 247 (1969); J. S. Rowlinson and P. I. Freeman, *ibid.* **1**, 20 (1960).
[71] B. Chu, I. H. Park, Q.-W. Wang, and C. Wu, Macromolecules **20**, 2833 (1987); I. H. Park, Q.-W. Wang, and B. Chu, *ibid.* **20**, 1965 (1987); K. Kubota, K. M. Abbey, and B. Chu, *ibid.* **16**, 137 (1983); J. F. Douglas, *ibid.* **21**, 3515 (1988).
[72] M. E. Fisher, Phys. Rev. Lett. **57**, 1911 (1986).
[73] Sanchez [I. C. Sanchez, J. Phys. Chem. **93**, 6983 (1989)] has suggested that the correlation length amplitude ξ_o of polymer solutions near the critical point correlates with the square root of the critical composition.